Effects of Thermal Imidization on Mechanical Properties of Poly(amide-*co*-imide)/Multiwalled Carbon Nanotube Composite Films

Seung Hwan Lee,[1] Sheong Hyun Choi,[2] Seong Yun Kim,[1] Jae Ryoun Youn[1]

[1]*Department of Materials Science and Engineering, Research Institute of Advanced Materials (RIAM), Seoul National University, Seoul 151-744, Korea*
[2]*The Technology Commercialization Center, Hyosung Corporation, Anyang-Si 431-080, Gyeonggi-Do, Korea*

Received 20 August 2009; accepted 26 January 2010
DOI 10.1002/app.32177
Published online 3 May 2010 in Wiley InterScience (www.interscience.wiley.com).

ABSTRACT: In this study, experimental and numerical studies were performed to investigate the relationship among the functionalization method, weight fraction of MWCNTs, thermal imidization cycle, and mechanical properties of various PAI/MWCNT composite films. Poly(amide-*co*-imide)/multiwalled carbon nanotube composite films were prepared by solution mixing and film casting. The effects of chemical functionalization and weight fraction of multiwalled carbon nanotubes on thermal imidization and mechanical properties were investigated through experimental and numerical studies. The time needed to achieve sufficient thermal imidization was reduced with increasing multiwalled carbon nanotube content when compared with that of a pure poly(amide-*co*-imide) film because multiwalled carbon nanotubes have a higher thermal conductivity than pure poly(amide-*co*-imide) resin. Mechanical properties of pure poly(amide-*co*-imide) and poly(amide-*co*-imide)/multiwalled carbon nanotube composite films were increased with increasing imidization time and were improved significantly in the case of the composite film filled with hydrogen peroxide treated multiwalled carbon nanotubes. Both the tensile strength and strain to failure of the multiwalled carbon nanotube filled poly(amide-*co*-imide) film were increased substantially because multiwalled carbon nanotube dispersion was improved and covalent bonding was formed between multiwalled carbon nanotubes and poly(amide-*co*-imide) molecules. © 2010 Wiley Periodicals, Inc. J Appl Polym Sci 117: 3170–3180, 2010

Key words: poly(amide-*co*-imide); imidization; carbon nanotubes; functionalization

INTRODUCTION

Carbon nanotubes (CNTs) have distinct nanostructures with remarkable properties due to their high aspect ratio and arrangement of carbon hexagons into tube-like fullerenes. They have been produced in single-walled, double-walled, or multiwalled nanotube structures and each type has distinct physical characteristics that make it suitable for end-user applications, e.g., optical components and polymeric composites because of their excellent properties on the nanometer scale. Polymer/CNT composites are of keen interest owing to their unique mechanical and multifunctional properties resulting from the high aspect ratio and large surface area of CNTs. However, CNTs tend to be aggregated and entangled together as a bundle, leading to many defects in CNT composites. Important problems on polymer/CNT composites are how to improve the dispersion of CNTs in the matrix and to increase interfacial bonding between the polymer matrix and CNTs through various chemical and physical methods.[1–3] According to recent reports,[4,5] the CNT treatments are made by modifying the covalent and noncovalent bonding formed between the polymer matrix and CNT surface. Covalent bonding is improved by a surface treatment, which disrupts the delocalized π-electron systems and then leads to incorporation with other species at the CNT surface. It is usually realized by oxidizing CNTs in an acid for attachment of carboxylic or hydroxy groups to the defect sites of CNTs. On the other hand, noncovalent bonding is realized by wrapping the CNTs with polymer resin via various interaction forces, e.g., van der Waal's force and π–π stocking interactions. Although the π–π stocking bonding between CNT sidewalls and functional groups is relatively weak and the load transfer is not high enough, noncovalent methods have been of interest because they provide possibilities of attaching many functional groups onto CNT sidewalls without disrupting its hexagonal atomic structure.[6,7]

Correspondence to: J. R. Youn (jaeryoun@snu.ac.kr).
Contract grant sponsor: Korea Science and Engineering Foundation (KOSEF) [Korean government (MEST), (ITRC)]; contract grant number: R11-2005-065.

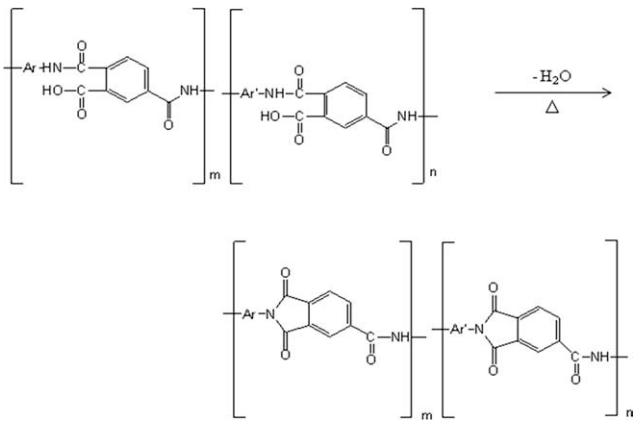

Scheme 1 Thermal imidization reaction of poly(amide-*co*-imide) used in this study.

Poly(amide-*co*-imide), PAI, shows outstanding characteristics, e.g., naturally nonflammable and thermally stable at high temperature, due to its chemical structure consisting of a high proportion of aromatic rings, double bonds, and heterocyclic imide structure along the polymer backbone.[8–16] Since it has polyamide and polyimide groups existing in the molecular backbone and carboxyl groups existing in the PAI precursor can induce hydrogen bonding, PAI resin becomes a promising candidate for matrix of hybrid composites.[17,18] Therefore, it has been widely used as filtration media, precision plastic parts, and reinforcements by exploiting its superior chemical resistance and mechanical properties at high temperature. PAI resin has also exceptional wear resistance with high strength as well as thermal and dimensional stability in both dry and wet environments. However, the crude PAI has weak, brittle, and poor chemical and wear resistance due to low molecular weight. As shown in Scheme 1, therefore, crude PAI resin should be converted into final products through imidization with thermal and chemical routes to achieve outstanding properties of final PAI products. As a preferable method, PAI resin has been imidized thermally because thermal process is more simple and economical than chemical process. It is also well known that the thermal imidization time and cycle are dependent on the thickness of the PAI product and its geometry.[19–21] Therefore, it is necessary to understand correlation between the thermal imidization cycle and physical properties of PAI products with different geometry to determine optimum thermal imidization conditions. However, it is hard to find studies about correlation between the thermal imidization time and inorganic fillers, e.g., multiwalled carbon nanotubes (MWCNTs) and layered silicates incorporated into the PAI resin.

In this study, PAI/MWCNT composite films were prepared with solution mixing, film casting, and compression molding. Experimental and numerical studies were carried out to investigate the relationship among the functionalization method, weight fraction of MWCNTs, thermal imidization cycle, and mechanical properties of the various PAI/MWCNT composite films. Especially, the difference in the thermal imidization time of the pure PAI and the PAI/MWCNT composite film was investigated in detail since the thermal imidization time of the PAI/MWCNT composite films may be different from that of the pure PAI film due to high thermal conductivity of the MWCNTs.

EXPERIMENTAL

Materials and chemical modification of MWCNTs

PAI resin (Torlon® PAI 4000-T HV, Solvay Advanced Polymers L.L.C, Alpharetta, GA) was supplied as powders and used as the matrix material in this study. As shown in Scheme 2, the PAI resin was imidized partially at temperature ranges of 90–110°C because it was difficult to use nonimidized PAI resin for film casting owing to hydrolysis due to water molecules existing in atmosphere. MWCNTs (Carbon Nano-materials Technology, Pohang, Korea) produced by the catalytic chemical vapor deposition method have the diameter of 5 to 20 nm, the length longer than 10 μm, and therefore the aspect ratio larger than five hundred. Specific surface area of the MWCNT measured by using the Brunauer-Emmett-Teller (BET) method ranged from 100 to 700 m^2/g. *N*-methyl-2-pyrrolidone (NMP) (Daejung Chemicals and Metals, Siheung, Korea) was used as a solvent to dissolve crude PAI precursor resin.

Chemical modification of the MWCNT surface was performed by three different methods, i.e., acid, hot air, and hydrogen peroxide treatments. Acid treatment was performed as follows. Firstly, MWCNTs were dispersed in a 65% solution of 3 : 1 mixture of H_2SO_4/HNO_3 in water. Then, the suspension was treated by ultrasonic excitation for 1 h at 80°C to attach carboxyl and hydroxyl groups onto the surface of MWCNTs. After acid treatment, the MWCNTs (a-MWCNTs) were cleaned several times with distilled water, filtered by using filtering paper with pore size of 1 μm, and then dried at 50°C in vacuum oven for 2 days. Hydrogen peroxide

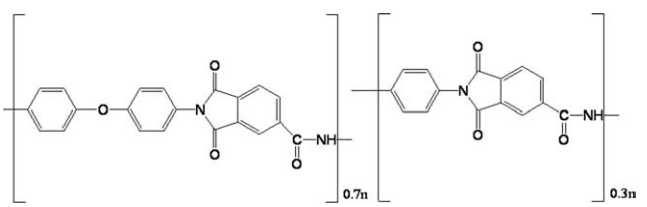

Scheme 2 Chemical structure of PAI resin powders used in this study.

TABLE I
Compositions of the PAI/MWCNT Composites Prepared by Solution Mixing

	Untreated MWCNT	Acid treated MWCNT	Heat treated MWCNT	Hydrogen peroxide treated MWCNT
PAI/CNT1.0	1.0 wt %	–	–	–
PAI/a-CNT1.0	–	1.0 wt %	–	–
PAI/h-CNT1.0	–	–	1.0 wt %	–
PAI/*p*-CNT0.5	–	–	–	0.5 wt %
PAI/*p*-CNT1.0	–	–	–	1.0 wt %
PAI/*p*-CNT1.5	–	–	–	1.5 wt %
PAI/*p*-CNT2.0	–	–	–	2.0 wt %

treatment was similar to the acid treatment. MWCNTs were dispersed in the 1 : 1 mixture of H_2O_2/distilled water. Then, the mixture was sonicated for 1 h at 80°C to generate carboxyl and hydroxyl groups onto the surface of MWCNTs. After hydrogen peroxide treatment, the mixture was cleaned several times with distilled water and filtered by using a paper with pore size of 1 μm. Hydrogen peroxide treated MWCNTs (*p*-MWCNTs) were dried at 50°C in vacuum oven for 2 days. Heat treatment was carried out by heating MWCNTs at 500°C for 1 h in a furnace with air circulation. The heat treated MWCNTs (h-MWCNT) were collected after the heat treatment.

Preparation of PAI/MWCNT composite films

Crude PAI powders were added into NMP to make crude PAI/NMP solution and the solution was mixed at 100°C for 1 day by using a mechanical agitator. Four types of PAI/NMP solutions, i.e., 10, 15, 20, and 25 wt %, were prepared. Then films were cast with four types of PAI/NMP solutions to determine which concentration was proper for film casting. Finally, PAI/NMP solution of 15 wt % was selected to cast film specimens. To make PAI/MWCNT composite film, four types of MWCNTs, i.e., untreated, acid, heat, hydrogen peroxide treated MWCNTs were dispersed in PAI/NMP solution under ultrasonication at room temperature for 2 h. Weight fraction of the *p*-MWCNTs in the PAI/*p*-MWCNT composite specimen was finally chosen to be 0.5, 1.0, 1.5, and 2.0 wt % as shown in Table I.

After PAI/NMP/MWCNT suspensions were prepared with different MWCNT concentrations, they were poured into a rectangular die surrounded by Teflon film. They were dried in a convection oven for 2 days at 80°C to remove the solvent and additional drying was conducted in a vacuum oven for 3 days at 40°C. Since thickness of each specimen was not uniform, compression molding was performed for 15 min at 150°C under 15 tons by using a hot press (Wabash Metal Products, Anaheim, CA). In this study, flat dog-bone-like mold with dimension of 110 × 18 × 0.4 mm^3 was used and final thickness of the film after compression molding was about 400 μm. To convert the crude PAI resin into final PAI films, PAI/MWCNT composite films were thermally imidized with various curing cycles as shown in Table II. Thermal imidization of the PAI/MWCNT composite specimen was carried out at 330°C in a furnace (L15/1100/P320, Nabertherm, Lilienthal, Germany) with air circulation.

Characterization

Functional groups which were created on the MWCNT surface were detected using Fourier transform infrared spectroscopy (FTIR, JASCO 660 Plus, JASCO, Tokyo, Japan) between 650 and 4000 cm^{-1} by using a potassium bromide pellet. Tensile properties of PAI/MWCNT composite films were measured by using a universal testing machine (5565, INSTRON, High Wycombe, UK). Tensile tests were carried out at room temperature with the crosshead speed of 0.5 mm/min and at least five specimens were tested for each PAI/MWCNT composite film. Tensile specimens were made by stamping the film by using a dog-bone shaped shearing die. Morphological properties were observed with a scanning electron microscopy (SEM, JSM-6390LV, JEOL, Tokyo, Japan) at high magnification (×30,000) to investigate dispersion of MWCNTs in PAI/MWCNT composite films. Fractured surfaces of tensile specimens were coated with gold in vacuum for 50 s by using a sputter coating machine (Sputter Coater-108, Cressington Scientific Instruments, Watford, UK) and then SEM observation was carried out at 25.0 kV.

TABLE II
Thermal Curing Cycles Applied to Pure PAI and PAI/MWCNT Composite Films

Total imidization time (hrs)	Preheating time (min)	Raising time (min)	Holding time (min)
No cure	–	–	–
6	10	145	205
9	10	220	310
12	10	295	415
18	10	440	630

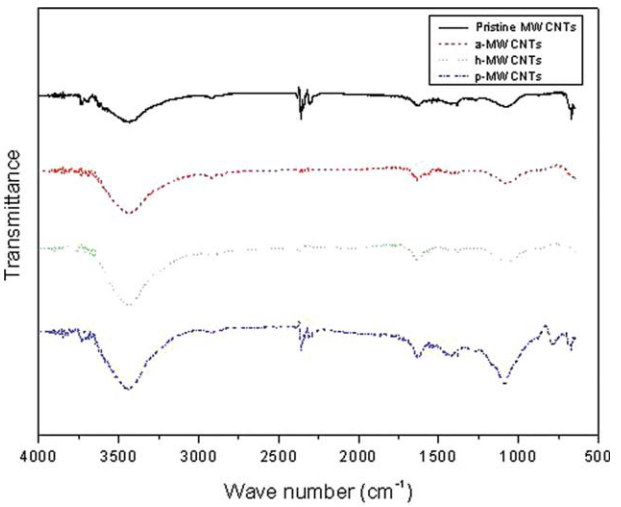

Figure 1 FTIR spectra of pristine, acid, heat, and hydrogen peroxide treated MWCNTs. [Color figure can be viewed in the online issue, which is available at www.interscience.wiley.com.]

RESULTS AND DISCUSSION

Chemical structure of surface treated MWCNTs

It is possible to identify functional groups from the characteristic peak position, width, and intensity of their FTIR spectra. As shown in Figure 1, a-MWCNTs show different peaks from the untreated MWCNTs. The broad peak around 3438 cm^{-1} is assigned to hydroxyl (O—H) groups, the peak around 1634 cm^{-1} is assigned to carbonyl (C=O) groups, and the very weak peak around 1072 cm^{-1} is assigned to carbon-oxygen single bond (C—O). It was found that hydroxyl and carbonyl groups were attached to the surface of MWCNTs as the result of acid treatment. In the case of the h-MWCNTs, characteristic peak band of the FTIR spectrum was similar to that of the a-MWCNTs but intensity of each peak was increased slightly when compared with that of the a-MWCNTs. Oxidation reaction occurred on the MWCNT surface during heat treatment in hot air of 500°C.[4,5] In the case of the *p*-MWCNTs, characteristic band was observed especially around 1089 cm^{-1} as shown in Figure 1. The peak is much stronger than the peaks of MWCNTs treated with previous two methods and indicates that many C—O single bonds were generated at the MWCNT surface during hydrogen peroxide treatment. Subsequently, hydrogen peroxide treatment is the most efficient method to generate various functional groups, e.g., hydroxyl, carbonyl, and carboxylic acid groups on the MWCNT surface.[1]

Morphological properties

Fractured surface of the PAI/MWCNT composite specimen was observed by using a SEM to examine dispersion of MWCNTs in the PAI matrix. In Figure 2(a)–(e), SEM images of pristine MWCNTs and PAI/MWCNT composites are exhibited. Firstly, Figure 2(a) shows a curly and aggregated form of untreated as-received MWCNTs, which was generated in individual MWCNTs due to strong van der Waals interaction. As shown in Figure 2(b), it was found that pristine MWCNTs existed as agglomerates in the PAI matrix since MWCNT particles were aggregated by the van der Waals interaction. The van der Waal's interaction between MWCNTs has larger value than conventional carbon fillers because MWCNTs have extremely large aspect ratio and surface area.[6,7] On the other hand, more uniform dispersion was observed in the case of PAI/MWCNT composite films filled with chemically modified MWCNTs as shown in Figure 2(c)–(e). Entangled MWCNTs were treated by ultrasonic excitation during chemical functionalization of MWCNTs with acid and hydrogen peroxide. It is also known that the functionalization methods can generate hydroxyl and hydrophilic groups that are compatible with the amic acid group in the PAI resin.[22] Therefore, chemically functionalized MWCNTs could be dispersed well in the PAI matrix because surface modified MWCNTs have stronger interaction with PAI molecules than the untreated MWCNTs.[4–7] As shown in Figure 2(c)–(e), especially, hydrogen peroxide treatment induced better dispersion of MWCNTs than acid or heat treatments as shown in the previous FTIR spectra.

SEM images of the composite films containing the *p*-MWCNTs are shown in Figure 3(a)–(d). In this study, PAI/*p*-MWCNT composites filled with *p*-MWCNTs of 0.5 and 1.0 wt % showed not only uniform and smooth fracture surface but also good dispersion of MWCNTs when compared with those of highly concentrated film specimens as shown in Figure 3(a,b). When the *p*-MWCNT content was below 1.0 wt %, entanglements were not observed and mechanical properties of the PAI/*p*-MWCNT composite films were improved. However, fracture surface of the PAI/*p*-MWCNT composite specimen became worse and many MWCNTs were pulled out from the fractured surface as the *p*-MWCNT content increased higher than 1.5 wt % as shown in Figure 3(c,d). As shown in all the SEM images, it was found that *p*-MWCNTs are randomly oriented in the PAI/*p*-MWCNT composites because the PAI/MWCNT solution was poured into the rectangular die and then compression molded after the film casting was completed.

Mechanical properties

Effects of imidization on mechanical properties of PAI/MWCNT composite films are plotted in Figures 4–7.

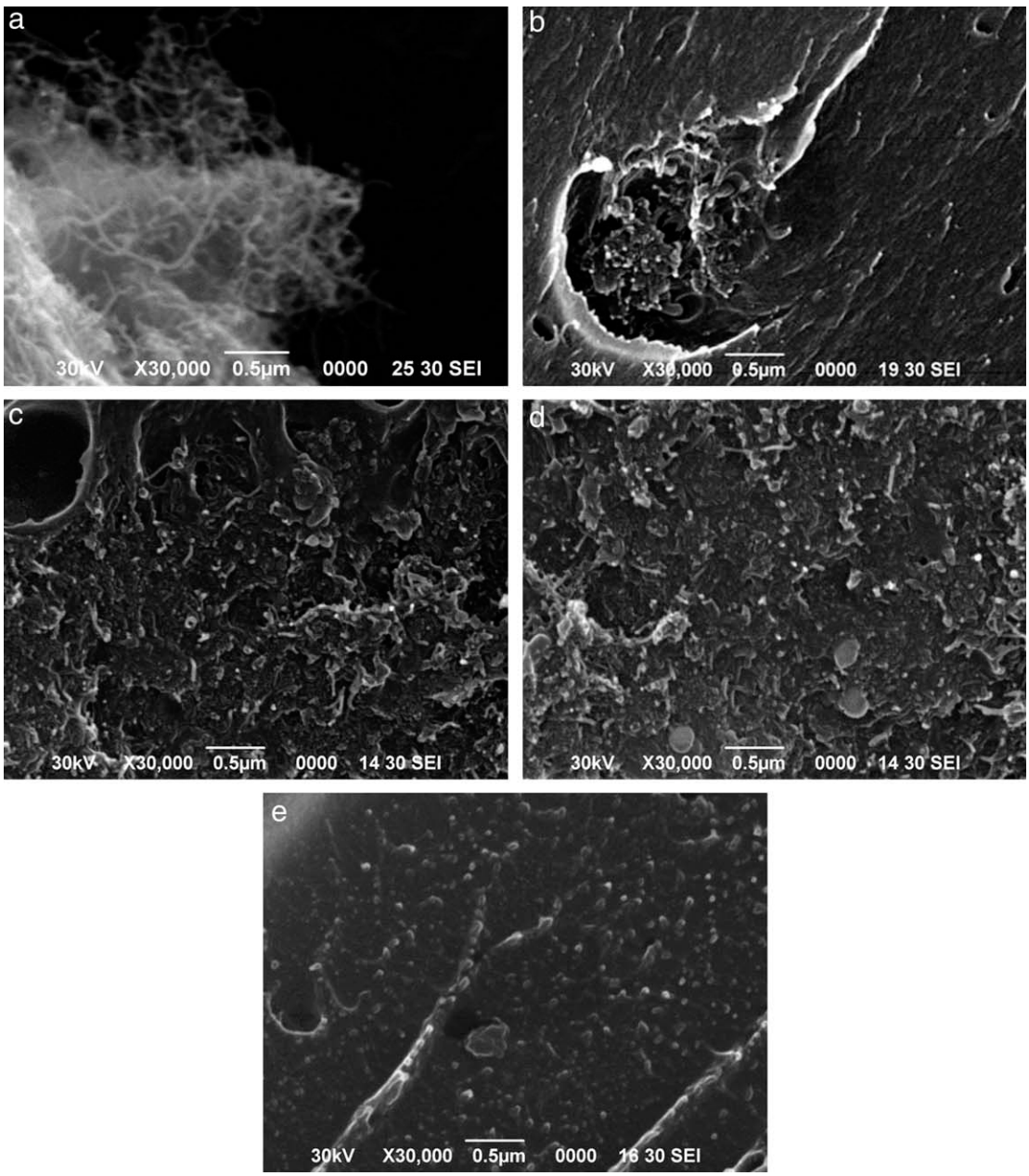

Figure 2 SEM images of (a) pristine MWCNTs and the fractured surface of PAI/MWCNT1.0 composite films containing (b) untreated MWCNTs, (c) acid treated MWCNTs, (d) heat treated MWCNTs, and (e) hydrogen peroxide treated MWCNTs of 1.0 wt %.

As shown in Figure 4(a,b), crude PAI film shows poor mechanical properties because it was not cured properly. However, mechanical properties of the PAI film were improved significantly with increasing thermal imidizaton time. In addition, both tensile stress and strain to failure were increased gradually for 12 h and then stayed at a plateau region. When thermal imidization of the tensile specimen was carried out for 12 h, it was found that sufficient imidization reaction occurred and crude PAI molecules were converted to final PAI molecules with heterocyclic imide rings in the PAI backbone where water was dehydrated.[23–25] In the case of PAI/*p*-MWCNT1.0 composite films, however, imidization time of about 9 h is enough to achieve perfect imidization of the crude PAI molecules because MWCNTs have higher thermal conductivity than the PAI matrix as shown in Figure 5(a,b). It is well known that composites with good dispersion of MWCNTs have a higher thermal conductivity than the pure polymer matrix.[26,27] Consequently, the experimental results showed that time needed to complete the imidization reaction was reduced slightly by incorporating MWCNT fillers into the PAI matrix.

Effects of MWCNT functionalization on mechanical properties of the composite films cured for 12 h are shown in Figure 6. Tensile strength and strain to

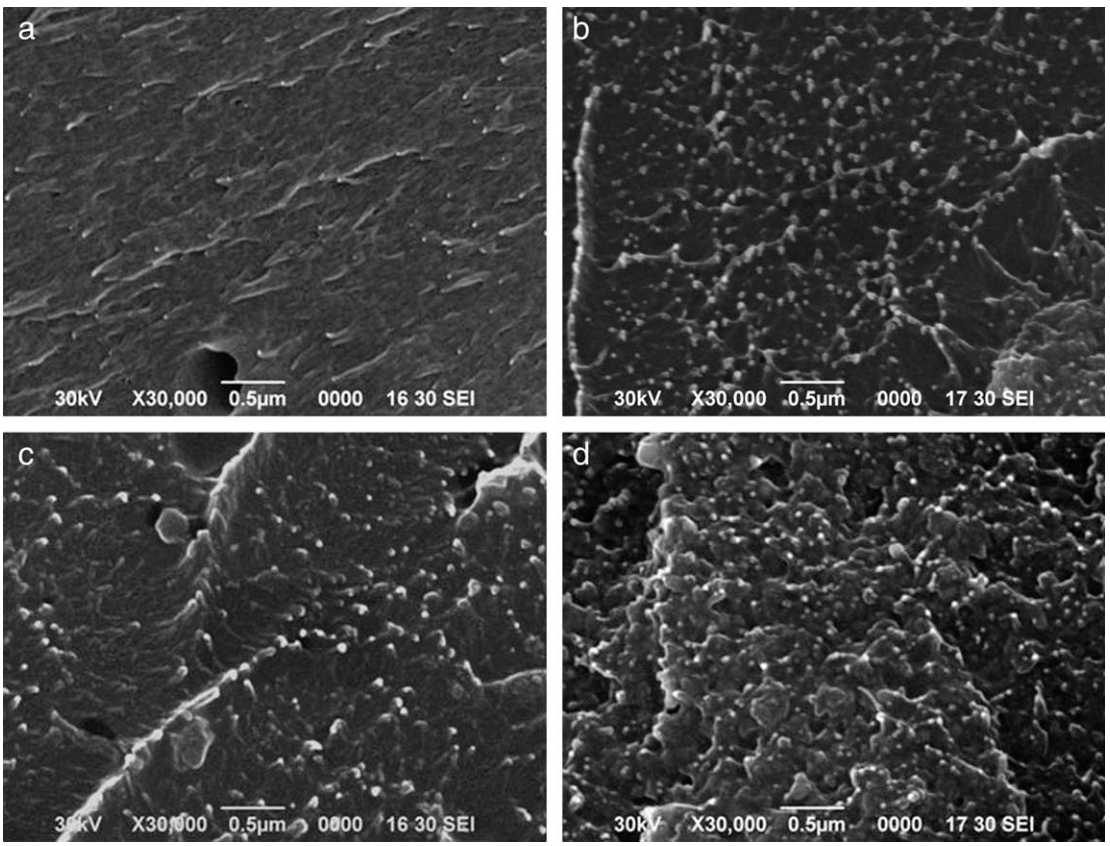

Figure 3 SEM images of the fractured surface of PAI/*p*-MWCNT composite films containing hydrogen peroxide treated MWCNTs of (a) 0.5 wt %, (b) 1.0 wt %, (c) 1.5 wt %, and (d) 2.0 wt %.

failure of the composites containing chemically functionalized MWCNTs were higher than those of pure PAI or untreated MWCNT filled PAI composite films because strong covalent bonding was formed between the functional groups generated on the surface of MWCNTs and the amic acid groups in PAI molecules.[4,5,9] Therefore, chemically functionalized MWCNT particles played an important role in the load transfer between MWCNTs and the PAI matrix. Especially, *p*-MWCNT filled PAI composite films showed the highest value among the PAI/MWCNT composite specimens. Superior mechanical properties of the PAI/*p*-MWCNT composite films were explained by FTIR and SEM results. Therefore, hydrogen peroxide treatment is the most effective method to reduce the imidization time and to increase covalent bonding between MWCNTs and PAI molecules in PAI/MWCNT composites.

As shown in Figure 7(a,b), tensile strength of the PAI/*p*-MWCNT composite specimen was gradually increased as the *p*-MWCNT content was increased up to 1.5 wt % and strain to failure was gradually increased as the *p*-MWCNT content was increased up to 1.0 wt %. Thereafter, both tensile strength and strain to failure were decreased because PAI/*p*-MWCNT composite films began to show transition from ductile to brittle behavior and *p*-MWCNTs were aggregated each other at the weight fraction of 1.5 to 2.0%. As shown in Figure 3, fractured surfaces of PAI/*p*-MWCNT composite specimens containing *p*-MWCNTs of 2.0 wt % showed aggregated MWCNTs due to relatively high filler content.[4,28–32]

To understand elastic modulus behavior with respect to MWCNT content in the PAI/MWCNT composite system, three types of models were investigated in this study. Firstly, the Halpin-Tasi model that has been widely used for prediction of the elastic modulus of polymeric comsposites was considered. Elastic modulus of a composite filled with aligned fillers, G_C, is given by the Halpin-Tasi model as below.[33]

$$G_C = G_P \frac{1 + \zeta \eta V_{\mathrm{CNT}}}{1 - \eta V_{\mathrm{CNT}}} \tag{1}$$

V_{CNT} is the volume fraction of MWCNTs, ζ is the shape parameter given by $\zeta = 2l/D$, and η is defined by the following equation.

$$\eta = \frac{G_{\mathrm{CNT}}/G_P - 1}{G_{\mathrm{CNT}}/G_P + 1} \tag{2}$$

where G_p and G_{CNT} are moduli of polymer and MWCNTs, respectively. On the other hand, a

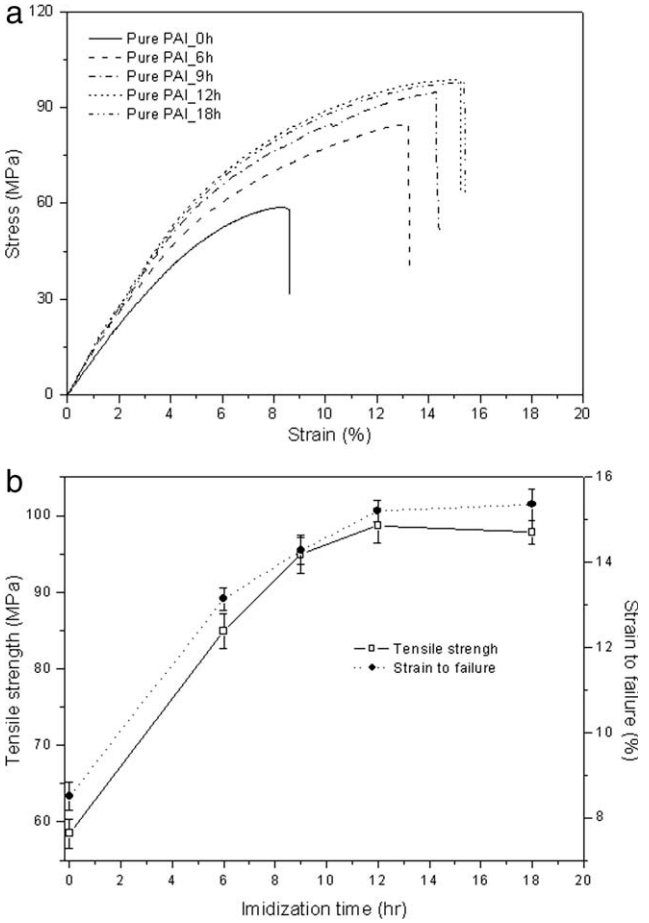

Figure 4 Effects of thermal imidization time on mechanical properties of pure PAI film: (a) stress–strain curve, (b) tensile strength and strain to failure as a function of imidization time.

modified model was suggested by Halpin and Kardos for calculating elastic modulus of polymer composites filled with randomly oriented fillers and the modulus can be expressed by the following Halpin-Kardos model.[34]

$$G_C = \frac{3}{8}\left[\frac{1+\zeta\eta_L V_{\mathrm{CNT}}}{1-\eta_L V_{\mathrm{CNT}}}\right]G_P + \frac{5}{8}\left[\frac{1+2\eta_T V_{\mathrm{CNT}}}{1-\eta_T V_{\mathrm{CNT}}}\right]G_P \quad (3)$$

where

$$\eta_L = \frac{G_{\mathrm{CNT}}/G_P - 1}{G_{\mathrm{CNT}}/G_P + \zeta} \text{ and } \eta_T = \frac{G_{\mathrm{CNT}}/G_P - 1}{G_{\mathrm{CNT}}/G_P + 2} \quad (4)$$

To compare predicted results with experimental data, constants of the models were determined, i.e., G_P is obtained from experimental data as 1.52 GPa, G_{CNT} is 1000 GPa, l/d is 100, and density of MWCNTs is 1.7 g/cm^3 as given by the references.[8,35–37]

As shown in Figure 8, elastic modulus of the PAI/*p*-MWCNT composites obtained experimentally was compared with predicted results as a function of *p*-MWCNT content ($V_{p\text{-CNT}}$). Elastic modulus of the PAI/*p*-MWCNT composite film was increased gradually with increasing *p*-MWCNT content. However, predicted results by the Halpin-Tasi model showed a large deviation when compared with experimental data because the Halpin-Tasi model assumed that the reinforcing fillers were aligned. On the contrary to the Halpin-Tasi model, the Halpin-Kardos model yielded good agreement with experimental data but there was still a difference between the Halpin-Kardos model and experimental data. The reason is that *p*-MWCNTs used in this study were not aligned but randomly oriented as shown in the previous SEM images. It is hard to achieve perfect interfacial adhesion or particle dispersion in polymer composites although it was assumed in the models that strong molecular interaction between fillers and polymer matrix as well as ideal dispersion of fillers existed in the polymeric composites. However, model prediction on elastic modulus of the PAI/*p*-MWCNT composite films gave similar results to experimental

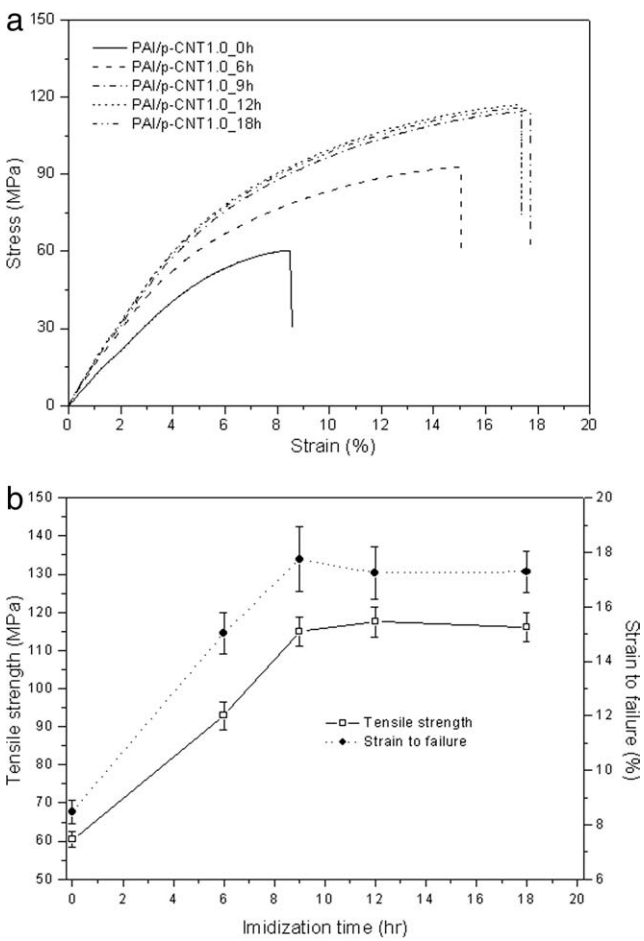

Figure 5 Effects of thermal imidization time on mechanical properties of PAI/*p*-MWCNT1.0 composite films: (a) stress–strain curve, (b) tensile strength and strain to failure as a function of imidization time.

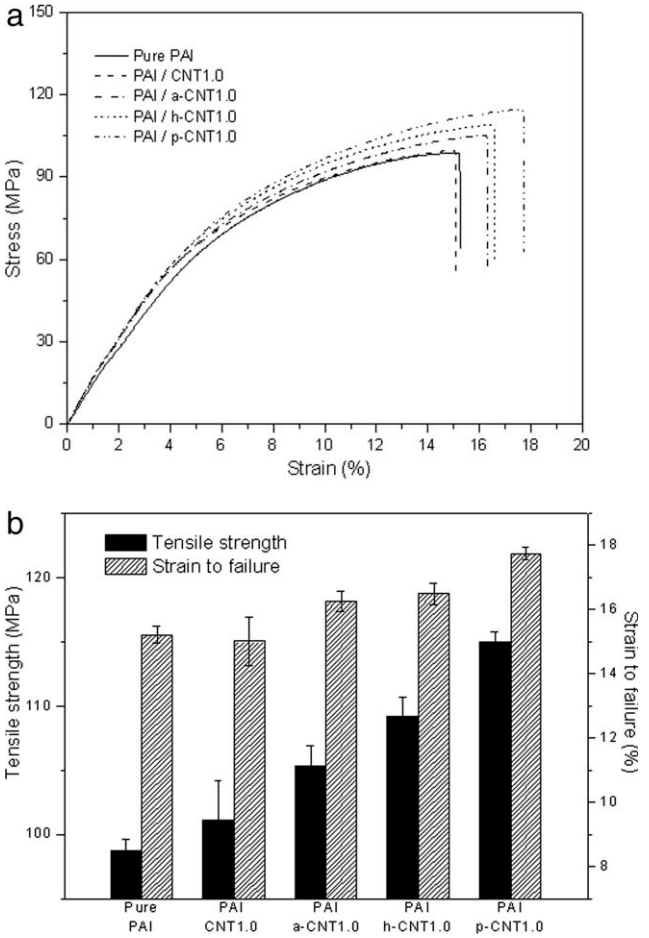

Figure 6 Effects of chemical functionalization of MWCNTs on mechanical properties of PAI/MWCNT composite films thermally imidized for 12 hours: (a) stress–strain curve, (b) tensile strength and strain to failure.

data. Therefore, it is concluded by the model prediction and experimental results that hydrogen peroxide treated MWCNTs provide good dispersion in the PAI matrix and induce good chemical bonding between *p*-MWCNTs and the functional groups of the PAI resin.

Heat transfer analysis was performed to comprehend difference of heat conduction between the pure PAI resin and PAI/MWCNT composites imidized for the same time. The purpose of the heat transfer analysis is to understand the temperature distribution in the PAI composite and the effect of temperature increase on the imidization which will influence development of mechanical properties of the cured composite specimens. It was shown by the mechanical properties that the imidizaton time of the pure PAI resin was longer than that of the PAI/*p*-MWCNT composite by about 3 h to complete thermal imidization. To understand this phenomenon, transient heat conduction analysis was performed along the thickness direction with proper convection boundary conditions by using the Comsol Multiphysics software program. Thermal conductivities of the pure PAI and PAI/*p*-MWCNT composite films were measured experimentally as 0.76 and 1.41 W/m K, respectively. Thermal conductivity effect at the edge region of the film was ignored because film thickness was much smaller than the length or the width.[38] Diagrams of the specimen, boundary conditions, and applied finite elements are illustrated in Figure 9.

Initial temperature at each position was set as 150°C and surrounding air temperature was set constant as 160°C. It was assumed that there was no radiation heat transfer. Heat transfer and heat generation in the film are governed by the following equation.[39]

$$\rho C_p \frac{\partial T}{\partial t} - \nabla \times (k \nabla T) = h(T_{\text{ext}} - T) \tag{5}$$

where ρ is the density of film (1.59 g/cm^3), C_P is the heat capacity of film (1.12 J/kg K), T is temperature of film as a function of time and position, k is the thermal conductivity measured experimentally, h is

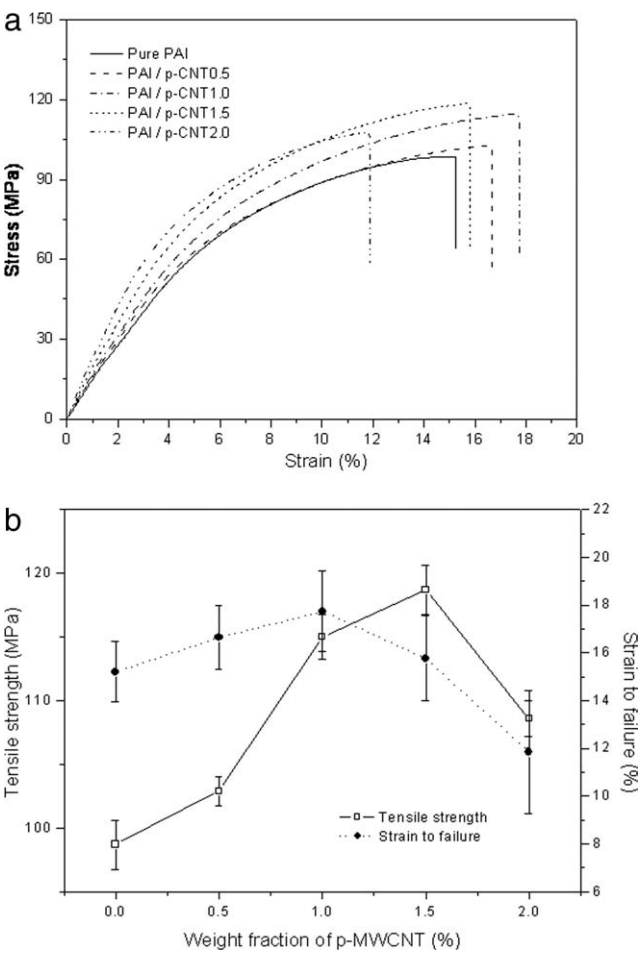

Figure 7 Effects of *p*-MWCNT content on mechanical properties of PAI/MWCNT composite films: (a) stress–strain curve, (b) tensile strength and strain to failure.

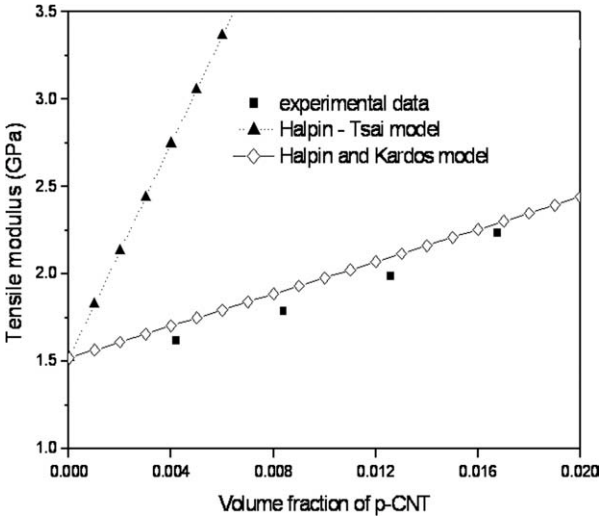

Figure 8 Tensile moduli of PAI/MWCNT composite films predicted by the Halpin-Tsai model and the Halpin-Kardos model compared with experimental data as a function of *p*-MWCNT volume fraction.

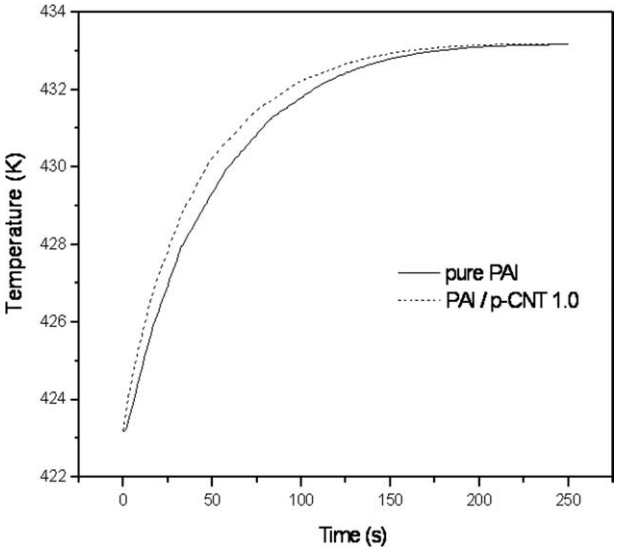

Figure 10 Temperature variation obtained by heat transfer simulation on pure PAI and PAI/*p*-MWCNT1.0 composite films.

the convection heat transfer coefficient (10 W/m^2 K), and T_{ext} is surrounding air temperature (160°C).[35–37] The convection boundary condition at the wall ($x = \pm 2 \times 10^{-4}$) used in this simulation is given by the following equation.

$$\hat{n} \times (k\nabla T) = h(T_{ext} - T) \quad (6)$$

where $\hat{n}$ is the outward normal vector at the wall.

Temperature predictions for the pure PAI and PAI/*p*-MWCNT1.0 composite films are shown in Figures 10 and 11. Temperature variation at the center ($x = 0$) of pure PAI and PAI/*p*-MWCNT1.0 composite films is predicted with respect to the thermal imidization time in Figure 10. Temperature at the center of the PAI/*p*-MWCNT1.0 composite film reached 160°C faster than that of the pure PAI film. The MWCNT filled specimen showed faster heat transfer than the pure PAI film because it has higher thermal conductivity. Temperature distribution predicted along with the thickness direction is shown in Figure 11(a,b). When temperature of the core region reached 159°C, 90% of the heat conduction is completed. For the pure PAI film, it takes 128 s until the temperature becomes 159°C and temperature distribution is not uniform along the thickness direction because of low thermal conductivity of the PAI resin. In the case of the PAI/*p*-MWCNT1.0 film, however, it takes 99 s to reach 159°C at the core region, which is faster than that of the pure PAI film. Furthermore, temperature distribution in the PAI/*p*-MWCNT1.0 composite film was more uniform than that in the pure PAI film. It was found that MWCNTs in the PAI matrix increased the thermal conductivity and contributed to uniform temperature distribution in the PAI/MWCNT composite film. Considering the experimental and predicted results on mechanical properties and thermal conduction, MWCNTs are effective in improving tensile strength and decreasing imidization time of the PAI resin.

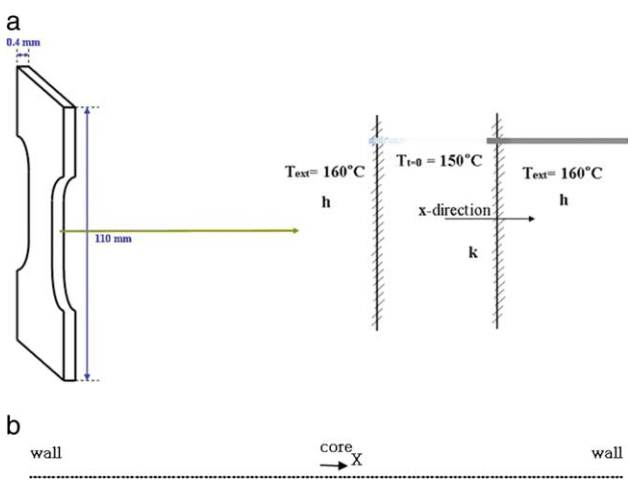

Figure 9 A schematic of (a) the sample with applied thermal boundary conditions and (b) 1D Lagrange quadratic mesh with 128 elements. [Color figure can be viewed in the online issue, which is available at www.interscience.wiley.com.]

CONCLUSIONS

PAI/MWCNT composite films were prepared by solution mixing and film casting to investigate effects of chemical functionalization and MWCNT fraction on thermal imidization behavior and mechanical properties of PAI/MWCNT composites. Three types

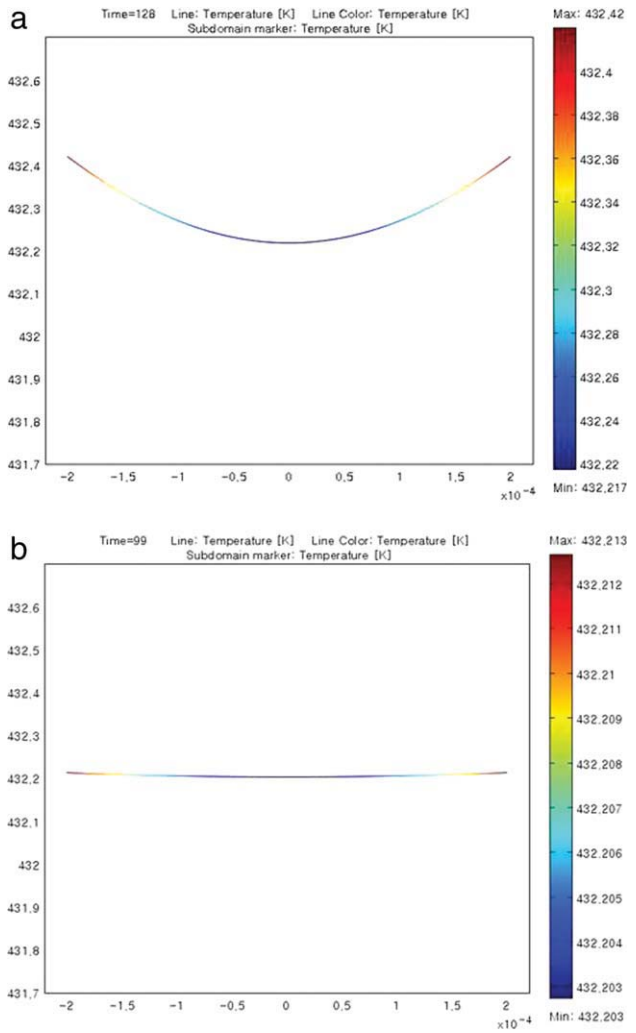

Figure 11 Predicted temperature distribution along with the thickness direction of (a) pure PAI and (b) PAI/*p*-MWCNT1.0 composite films when the core region reaches 432.2 K. [Color figure can be viewed in the online issue, which is available at www.interscience.wiley.com.]

of chemical functionalization methods, i.e., acid, hot air, and hydrogen peroxide treatments were used in this study. Hydrogen peroxide treatment was the most efficient method to generate various functional groups on the MWCNT surface, e.g., hydroxyl, carbonyl, and carboxylic acid groups. When the MWCNT content was below 1.0 wt %, entanglements were not observed and uniform dispersion was obtained. Mechanical properties of both pure PAI and PAI/MWCNT composite films were increased with increasing thermal imidization time. Especially, thermal imidization time of the PAI/*p*-MWCNT composite film was decreased by about 3 h when compared with that of the pure PAI film because of the high thermal conductivity and good dispersion of *p*-MWCNTs. It was found by the transient heat conduction analysis that the thermal conductivity of the MWCNT filled PAI matrix was increased and uniform temperature distribution was obtained in the PAI/MWCNT composite film. The PAI/*p*-MWCNT composite film showed the most promising results among PAI/MWCNT composite films filled with chemically functionalized MWCNTs. Both tensile strength and strain to failure of the MWCNT filled PAI film were increased substantially. In conclusion, the MWCNT reinforcement is effective in improving tensile strength and decreasing imidization time of the PAI resin.

References

1. Sung, Y. T.; Han, M. S.; Song, K. H.; Jung, J. W.; Lee, H. S.; Kum, C. K.; Joo, J.; Kim, W. N. Polymer 2007, 47, 4434.
2. Lee, S. H.; Kim, M. W.; Kim, S. H.; Youn, J. R. Eur Polym J 2008, 44, 1620.
3. Salvetat, J. P.; Briggs, A. D.; Bonard, J. M.; Bacsa, R. R.; Kulik, A. J.; Stockli, T.; Burnham, N. A.; Forro, L. Phys Rev Lett 1999, 82, 944.
4. Kim, J. A.; Seong, D. G.; Kang, T. J.; Youn, J. R. Carbon 2006, 44, 1898.
5. Lee, S. H.; Cho, E. N. R.; Jeon, S. H.; Youn, J. R. Carbon 2007, 45, 2810.
6. Eitan, A.; Jiang, K.; Dukes, D.; Andrews, R.; Schadler, L. S. Chem Mater 2003, 15, 3198.
7. Song, Y. S.; Youn, J. R. Carbon 2005, 43, 1378.
8. Margolis, J. M. Engineering Plastics Handbook; McGraw-Hill: New York, 2006.
9. Robertson, G. P.; Guiver, M. D.; Yoshikawa, M.; Brownstein, S. Polymer 2004, 45, 1111.
10. Mehdipour-Ataei, S.; Hatami, M. Eur Polym J 2005, 41, 2010.
11. Liaw, D. J.; Chang, F. C.; Liu, J. H.; Wang, K. L.; Faghihi, K.; Huang, S. H.; Lee, K. R.; Lai, J. Y. Polym Degrad Stab 2007, 92, 323.
12. Choi, N. S.; Yew, K. H.; Choi, W. U.; Kim, S. S. J Power Sources 2008, 177, 590.
13. Liu, Z.; Guo, Q.; Shi, J.; Zhai, G.; Liu, L. Carbon 2008, 46, 414.
14. Yang, C. P.; Chen, R. S.; Wei, C. S. Eur Polym J 2002, 38, 1721.
15. Yang, C. P.; Liou, G. S.; Yang, C. C.; Chen, S. H. Polym Bull 1999, 43, 21.
16. Thirunavukkarasu, A.; Nanjan, M. J. Polym J 1983, 15, 855.
17. Ranade, A.; D'souza, N. A.; Gnade, B. Polymer 2002, 43, 3759.
18. Buch, P. R.; Mohan, D. J.; Reddy, A. V. R. Polym Int 2006, 55, 391.
19. Ghosh, M. K.; Mittal, K. L. Polyimide: Fundamentals and Applications; Marcel Dekker: New York, 1996.
20. Peng, N.; Chung, T. S.; Lai, J. Y. J Membr Sci 2009, 326, 608.
21. Stevens, M. P. Polymer Chemistry: An Introduction; Oxford University Press: Oxford, 1999.
22. Feng, Q. P.; Xie, X. M.; Liu, Y. T.; Zhao, W.; Gao, Y. F. J Appl Polym Sci 2007, 106, 2413.
23. Zhai, Y.; Yang, Q.; Zhu, R.; Gu, Y. J Mater Sci 2008, 43, 338.
24. Yu, K. H.; Yoo, Y. H.; Rhee, J. M.; Lee, M. H.; Yu, S. C. Mat Res Innovat 2003, 7, 51.
25. Mohsin, M. A.; Akhter, Z.; Bolte, M.; Butt, M. S.; Khan, M. S. U.; Siddiqi, M. H. J Mater Sci 2009, 44, 4796.
26. Cai, H.; Yan, F.; Xue, Q. Mater Sci Eng A 2004, 364, 94.
27. Vigolo, B.; Mamane, V.; Valsaque, F.; Le, T. N. H.; Thabit, J.; Ghanbaja, J.; Aranda, L.; Fort, Y.; Mcrae, E. Carbon 2009, 47, 411.
28. Cha, S. I.; Kim, K. T.; Lee, K. H.; Mo, C. B.; Jeong, Y. J.; Hong, S. H. Carbon 2008, 46, 482.
29. Sun, L.; Warren, G. L.; O'reilly, J. Y.; Everett, W. N.; Lee, S. M.; Davis, D.; Lagoudas, D.; Sue, H. J. Carbon 2008, 46, 320.

30. Nielsen, L. F. Composite Materials: Properties as Influenced by Phase Geometry; Springer: Berlin, 2005.
31. Yung, K. C. J Reinf Plast Comp 2006, 25, 847.
32. Hull, D.; Clyne, T. W. An Introduction to Composite Materials; Cambridge University Press: New York, 1996.
33. Ramakrishna, S.; Lim, T.; Inai, R.; Fujihara, K. Mech Adv Mater Struc 2006, 13, 77.
34. Halpin, J. C.; Kardos, J. L. Polym Eng Sci 1976, 16, 344.
35. Mark, J. E. Polymer Data Handbook; Oxford University Press: Oxford, 1999.
36. Yoshikawa, M.; Guiver, M. D.; Robertson, G. P. J Mol Struct 2005, 739, 41.
37. Lee, S. H.; Kim, J. H.; Choi, S. H.; Kim, S. Y.; Kim, K. W.; Youn, J. R. Polym Int 2009, 58, 354.
38. Clancy, T. C.; Gates, T. S. Polymer 2006, 47, 5990.
39. Pitts, D. R.; Sissom, L. E. Theory and Problems of Heat Transfer; McGraw-Hill: New York, 1998.